International Conference on Mathematics, Computational Methods & Reactor Physics (M&C 2009)
Saratoga Springs, New York, May 3-7, 2009, on CD-ROM, American Nuclear Society, LaGrange Park, IL (2009)

EXPERIENCE IN THE USE OF THE MONTE-CARLO CODE BASED TRACING ALGORITHM AND THE VOLUME FRACTION METHOD IN VVER RADIATION SHIELDING CALCULATIONS

Michael I. Gurevich, Sergei M. Zaritsky, Dmitry S. Oleynik, Valentin V. Sinitsa
RRC Kurchatov Institute
Moscow, 123182, Kurchatov Sq., 1, Russia
gurevich@adis.vver.kiae.ru; zaritsky@adis.vver.kiae.ru; oleynik@adis.vver.kiae.ru;
vvs@dhtp.kiae.ru

Alexander A. Russkov, Andrei M. Voloschenko
Keldysh Institute of Applied Mathematics
Moscow, 125047, Miusskaya Sq., 4, Russia
russkov@inbox.ru; volosch@kiam.ru

Vladimir I. Tsofin, Alexander D. Djalandinov
OKB Gidropress
Podolsk, 142103, Ordzhonikidze Str., 21, Moscow Region, Russia
tsofin@grpress.podolsk.ru

Gennady N. Manturov
Institute of Physics and Power Engineering
Obninsk, 249033, Bondarenko Sq., 1, Kaluga Region, Russia
mant@ippe.ru

ABSTRACT

Monte-Carlo code based tracing algorithm is applied for converting combinatorial presentation of the problem geometry and source to a bit-mapped one with local conservation both the mass of original materials and the source yield for every spatial cell of the mesh. To make this transformation the volume fractions (VF) of original materials and source by spatial cells of the user supplied mesh are calculated by the tracing algorithm and the VF method is applied by introducing additional mixtures for spatial cells, where a few original materials are included. The use of the tracing algorithm makes this procedure fast and efficient. Received geometry and source approximation on the mesh ensures some improvement in convergence with mesh refinement. It also requires only minor changes in S_N transport codes, working with regular orthogonal meshes. Developed approach is tested in an example of VVER-1200 radiation shielding calculations.

Key Words: geometry approximation on the mesh, tracing algorithm, volume fraction method

1. INTRODUCTION

The problem of construction of efficient approximations of both core and radiation shielding geometry on the mesh seems of current interest. Probably, an optimal solution of this problem

can be received by the use of unstructured meshes [1]. But it seems that there is a more simple solution of the problem, based on the use of the volume fraction (VF) method, being applied to regular orthogonal meshes. In the VF method additional mixtures are introduced for spatial cells where a few original materials are available to ensure the local mass balance conservation. So, in this approach the homogenization procedure is applied for spatial cell volume and its error can be decreased to an acceptable level by the mesh refinement. This approach is not as accurate, as based on introducing of unstructured meshes, but due arithmetical simplicity and improved convergence properties can be also efficiently applied for solving complicated heterogeneous problems. It is also important that implementation of the VF method requires only minor changes in S_N transport codes, working with regular orthogonal meshes.

Known results in applying the VF method for solving the C5G7 MOX problem [2, 3, 4] and more realistic full core problems [5, 6], where about 50% of spatial cells or more contain additional mixtures of original materials, have demonstrated an acceptable performance of the VF method. On the other hand, if the local mass balance is not supported, then convergence in solving full core problems is very slow and a huge spatial mesh is required to receive acceptable accuracy. In solving radiation shielding problems, which are typically less heterogeneous than full core problems, the portion of additional mixtures for well organized spatial mesh is essentially less (about 5-10%). Numerical experiment has shown that in this case some improvement in geometry approximation and convergence due the local mass balance conservation also takes place.

A number of algorithms can be applied for calculations of the volume fractions of original materials by spatial cells of the mesh that overlays problem geometry starting with unstructured grids created using ICEM CFD Engineering grid generation tools [2] and finishing the simple refinement of the spatial mesh used, implemented in the BOT3P-5.1 code [7, 8]. The tracing algorithm is usually used in Monte-Carlo codes to calculate volumes of the bodies, included in the problem geometry. We have found that Monte-Carlo code based tracing algorithm, as it is available in the geometrical module of MCU code [9, 10], can be also used as a natural tool to calculate volume fractions fast and efficiently. The tracing algorithm can be also used to calculate by pin or by assembly defined source yield by spatial cells of the mesh.

The use of the same geometry/source input by MCU [9] and 3D S_N code KATRIN [10] gives an opportunity to perform both Monte-Carlo and S_N transport calculations with the use of the same geometry/source model of the problem solved. This also simplifies implementation of the CADIS methodology [11] for using the 3D S_N adjoint fluxes for automatic variance reduction of Monte-Carlo calculations through source biasing and consistent transport biasing with the weight window technique.

2. CALCULATION OF THE VOLUME FRACTIONS

The tracing algorithm is implemented for 2D x, y, r, z and r, ϑ, and 3D x, y, z and r, ϑ, z geometry models of the problem solved in the combinatorial geometry converter ConDat (Conversion of Data) [10] and for 3D x, y, z and r, ϑ, z geometries in the combinatorial source converter ConSource (Conversion of Source), which were developed on the base of the

geometrical module of the Monte-Carlo MCU code [9, 10] for solving transport equation. To ensure desirable accuracy the double precision arithmetic is used in these converters.

In ConDat code to calculate volume fractions of materials in cells of the mesh that overlays problem geometry, the path lengths in the original materials along the rays, which are traced (with a sufficient density) in parallel to x coordinate axis for Cartesian x, y and x, y, z geometries, and to r coordinate axis for curvilinear r, z, r, ϑ and r, ϑ, z geometries, are calculated. Monte-Carlo code is able to make this procedure fast. Using these data it is possible to calculate the contribution of any trajectory segment related volume to the material volume fractions in a spatial cell, as depicted in Fig. 1.

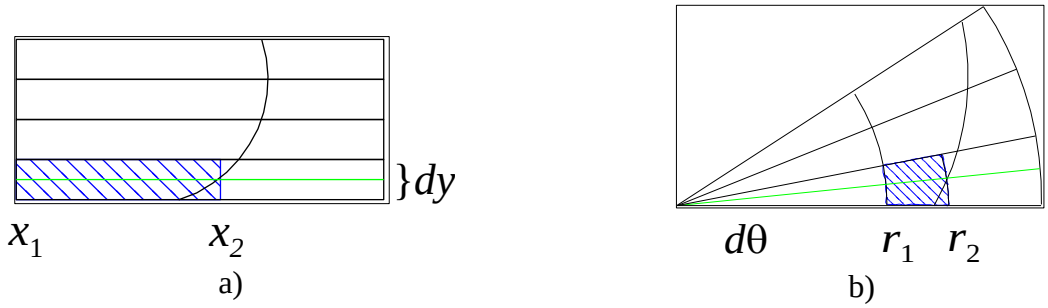

Figure 1. Calculation of the trajectory segment related volume yield to the material volume fractions in a spatial cell for x, y and r, ϑ geometries.

To control the accuracy of the material volume fractions obtained, the total material volumes are calculated. The received accuracy in calculation of these quantities can be used as a criterion of sufficiency of tracing ray density chosen. The ConDat code writes the calculated geometry presentation on the mesh in the *mixmap* format that is defined in the BOT3P-5.1 code manual [8]. Additional interface utility is available that transforms the *mixmap* format to the *matmap* one [8], where only original materials are available. In this transformation an additional mixture for a cell is replaced by the original material that gives maximum contribution to the cell material content. In *matmap* format only global conservation of mass of original materials may be supported by introducing density correction factors.

Similar geometry approximations can be also prepared by the BOT3P-5.1 code [7, 8], but the tracing algorithm seems as a more efficient method for calculation of volume fractions in comparison with the mesh refinement one, implemented in the BOT3P-5.1. In mesh refinement algorithm the material map for a very fine spatial mesh, received by a subdivision of spatial intervals of the original spatial mesh in every spatial variable available in a sufficiently large number of subintervals, is required. This work is essentially more expensive due a huge value of cells of a fine spatial mesh required to receive desired accuracy. For comparison, in the tracing algorithm the refinement of tracing rays is required only in 1 or 2 spatial variables for 2D and 3D geometry case, respectively.

3. VVER-1200 RADIATION SHIELDING CALCULATION BY THE VF METHOD

The applicability of the discussed geometry and source approximations was studied in an example of the VVER-1200 (that is under construction) radiation shield calculations, both 3D,

performed by S_N code KATRIN [10], and approximate synthetic, performed with the use of 1D and 2D S_N codes ROZ-6.6 [10] and KASKAD-S [10]. We note here that both ConDat and ConSource converters also support geometry and source preparation on the mesh for the synthesis method.

Some improvements in numerical algorithms [12], implemented in KATRIN code, which are essential for code performance in solving this problem: the cyclic through-computations method for solving two-point systems with periodic boundary conditions and an improved choice of the splitting-up algorithm parameters used to solve the P_1SA system for acceleration corrections, consistent with the WDD scheme, are published in [13].

A variant of the AWDD scheme with the fix-up function, which provides softer fix-up due continuity both the fix-up function and the first derivative of the fix-up function at the starting point of the fix-up [12, 13], is used in VVER-1200 calculations. This type of the fix-up function requires slightly more arithmetic operations in a cell calculation, but improves performance of the P_1SA scheme. Numerical experiment has shown that if the condition of continuity of the first derivative of the fix-up function is not satisfied, then the fix-up algorithm may (but quite seldom) generate instability in inner iterations convergence in solving 3D problems.

In performing accelerated up-scattering iterations in thermal region it is useful to vary accuracy of inner iterations convergence in dependence of achieved convergence of up-scattering iterations. Let ε and ε_{upsc} are the user defined group scalar flux point-wise accuracy of inner and up-scattering iterations convergence, respectively. Typical choice is: $\varepsilon = 10^{-3}$, $\varepsilon_{upsc} = 5 \cdot 10^{-3}$. Let $\varepsilon_{upsc}^{(s)}$ is the accuracy of up-scattering iterations achieved at the s-th up-scattering iteration, $s = 0,1,\ldots$. Then the accuracy of inner iterations convergence $\varepsilon^{(s+1)}$ for the $(s+1)$-th up-scattering iteration is calculated by the following formula, implemented in KATRIN code:

$$\varepsilon^{(s+1)} = \begin{cases} 10^{-1}, & s = 1 \\ \max\left(\varepsilon, \varepsilon_{upsc}\right), & \varepsilon_{upsc}^{(s)} > 10 \\ \varepsilon, & 10^{-1} < \varepsilon_{upsc}^{(s)} < 10 \\ \min\left(\varepsilon, 10^{-1}\varepsilon_{upsc}\right), & \varepsilon_{upsc}^{(s)} < 10^{-1} \end{cases} .$$

Decreasing of ε for the first up-scattering iteration is justified by strongly heterogeneous nature of a nonconverged thermal up-scattering source for this iteration that can essentially increase number of inner iterations required for convergence.

3.1. VVER-1200 Radiation Shielding Geometry and Source Approximation

The 3D combinatorial model of the VVER-1200 (that is under construction) radiation shield, prepared with the use of the MCU code geometrical module and MCU Viewer [9, 10] that is able to test MCU input, is depicted in axial and transverse sections in Figs. 2 through 5[1]. In radial

[1] Due limitation in number of colors to be displayed (16) in the current version of MCU Viewer, some material boundaries are not visible on the figures.

direction it includes core (375.0 cm in height), baffle (with external radius 173.5 cm), 1 cm water gap, 6.5 cm barrel, 30.6 cm downcomer (181.0 to 211.6 cm), 0.9 cm cladding, 19.75 cm reactor pressure vessel (RPV), 31.75 cm air cavity, 12 cm insulation, concrete dry shield that includes channels for thermal flux ionization chambers. (For comparison, for VVER-1000 the core height is 355.0 cm; downcomer, cladding and RPV thicknesses are 25.7, 0.8 and 19.25 cm, respectively). Two three floor assemblies (per 60° rotation symmetry sector) with surveillance specimens are located at theta angles $\vartheta_1 = 8.25°$ and $\vartheta_2 = \vartheta_1 + 43.5° = 51.75°$ in some distance from the inner boundary of RPV. The bottom and top reflectors are also included in the model. Approximation on the mesh of the 3D model of the VVER-1200 radiation shield in axial and transverse sections is depicted in Figs. 6 and 7. The CPU time of ConDat code, required to convert by the tracing algorithm the combinatorial presentation of the problem geometry on the r, ϑ, z spatial mesh that consists of 218×120×175 = 4 578 000 spatial cells with the use of 60 and 25 tracing rays per ϑ and z variable intervals, respectively, is 7 min 43 sec for Intel Core 2 Duo E6750 PC. 231352 additional mixtures (about 5% of total amount of spatial cells), used by the VF method, were created.

Combinatorial source for MCU code, based on by pin or (and) by assembly burnup data, calculated by PERMAK and BIPR codes, respectively, for some sequence of VVER-type reactor companies, can be prepared by specially designed utility BurnDat. In Fig. 8 the transverse sections at z=6.23 cm from the core bottom of the combinatorial by pin defined fission neutron density distribution, averaged over the VVER-1200 8-th (stationary) company period is depicted. This distribution was prepared by BurnDat code on the base of by pin burnup data, calculated by PERMAK code, and accounts for the dependence of the fission neutron multiplicity on the fuel burnup.

In Fig. 9 the same fission neutron density distribution, but converted on the spatial mesh by ConSource code with conservation of the local neutron yield (and additionally averaged by spatial cell volume), is depicted. The CPU time of ConSource code, required to convert by the tracing algorithm by pin defined combinatorial fission neutron density distribution on the mesh with the use of 60 tracing rays per interval in ϑ variable, is only 29 sec for Intel Core 2 Duo E6750 PC. To account for the axial distribution of the burnup, uniform spatial mesh of 30 spatial intervals is used in PERMAK code. Due the special type of combinatorial source used (by pin source form is not changed in core height), it is sufficient to perform tracing only for a single transverse section of the source.

Result of calculations essentially depends on accuracy of source approximation. The use of the by assembly defined source (Fig. 10), prepared by BurnDat code on the base of by assembly burnup data, calculated by the BIPR code (with practically the same by assembly yield of fission neutrons as for by pin defined one (Fig. 9)), and converted on the mesh by ConSource code, essentially overestimates fluxes in vicinity of RPV (see Fig. 11) and consequently, is not acceptable. (Here and below the problem dependent BGL1000 cross-section library [14] with 47 neutron and 20 photon groups that accounts for neutron thermalization was used for VVER-1200 radiation shielding calculations). Really, in this case by pin defined source for a peripheral assembly that is the sufficiently strongly varied one (by pin defined company burnup can decrease from pins located closely to core centre to external ones about three times) is replaced by a flat source for this assembly.

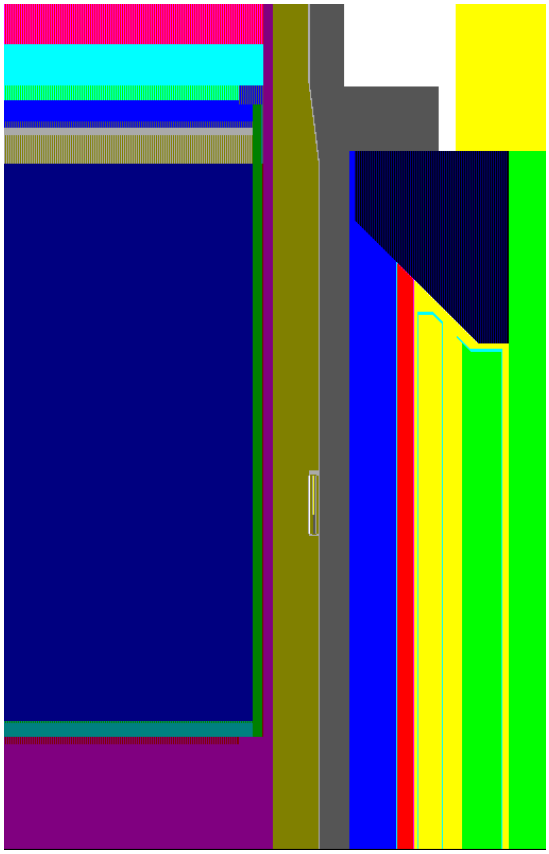

Figure 2. Axial section of the 3D r, ϑ, z VVER-1200 radiation shield geometry model for $\vartheta = 8.25°$. 3D problem geometry was prepared with the use of the combinatorial geometry approach and visualized by the MCU Viewer.

Figure 3. Longitudinal section for $\vartheta = 8.25°$ of the surveillance specimen assembly in the vicinity of the inner RPV surface of the VVER-1200 radiation shield.

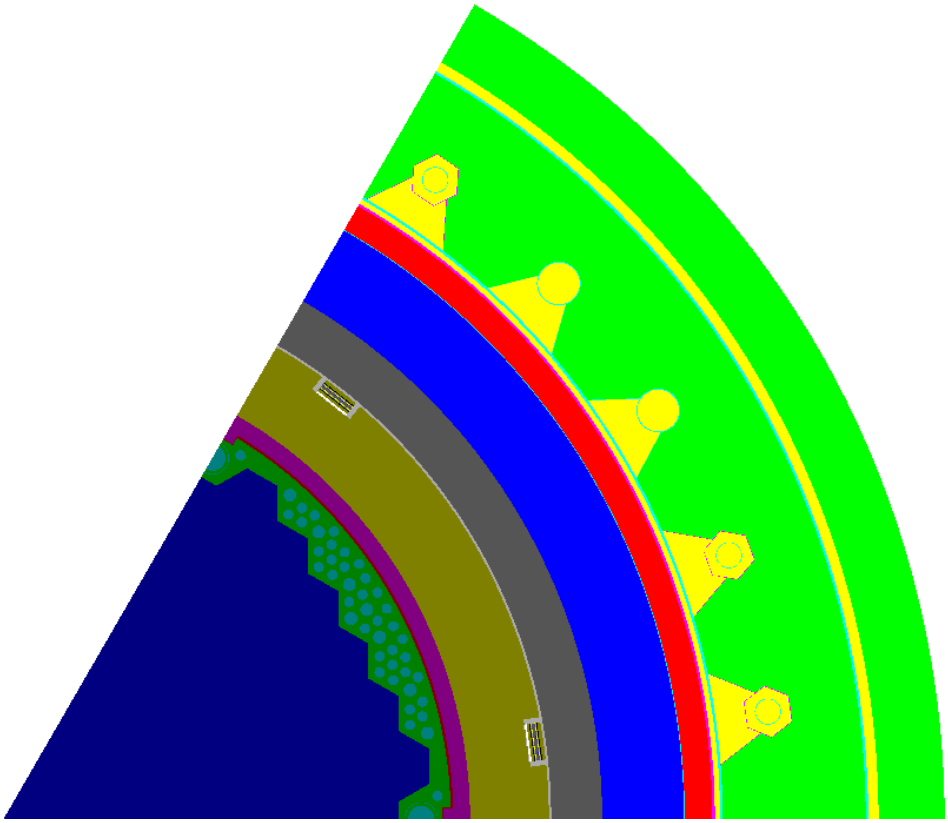

Figure 4. Transverse section of the 3D r, ϑ, z VVER-1200 radiation shield geometry model at $z = 220$ cm (130.9 cm from the bottom of the core).

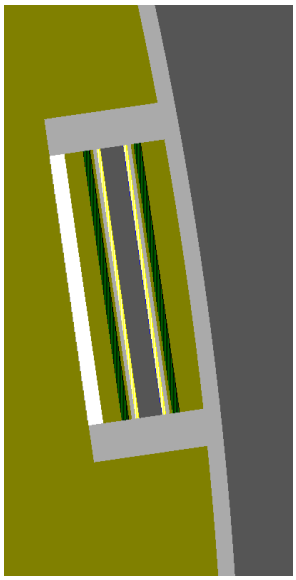

Figure 5. Transverse section of the surveillance specimen assembly in the vicinity of the RPV of the VVER-1200 radiation shield at $z = 220$ cm (130.9 cm from the bottom of the core).

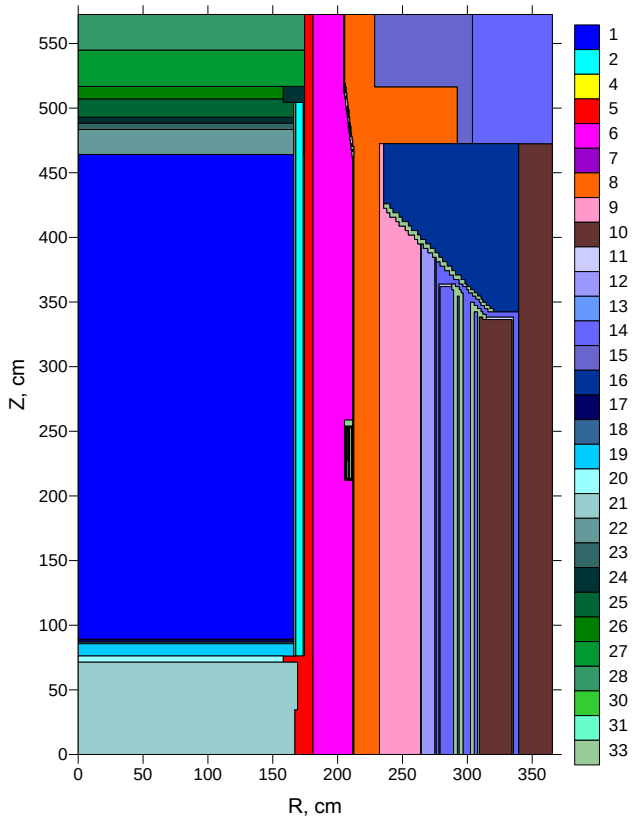

Figure 6. The VVER-1200 radiation shield 3D r,ϑ,z geometry model approximation on r,z 218×175 spatial mesh for axial section $\vartheta = 8.25°$, prepared by the ConDat converter. Additional mixtures generated are marked as the 33-th material.

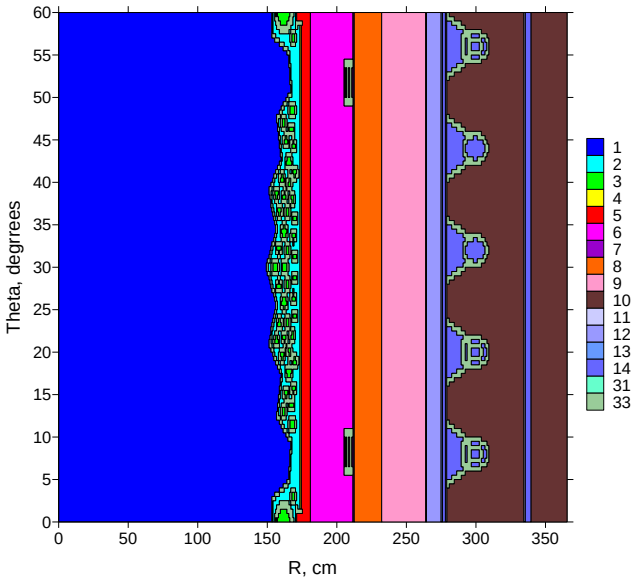

Figure 7. The VVER-1200 radiation shield 3D r,ϑ,z geometry model approximation on r,ϑ 218×120 spatial mesh for transverse section $z = 220$ cm (130.9 cm from the core bottom), prepared by the ConDat converter. Additional mixtures are marked as the 33-th material.

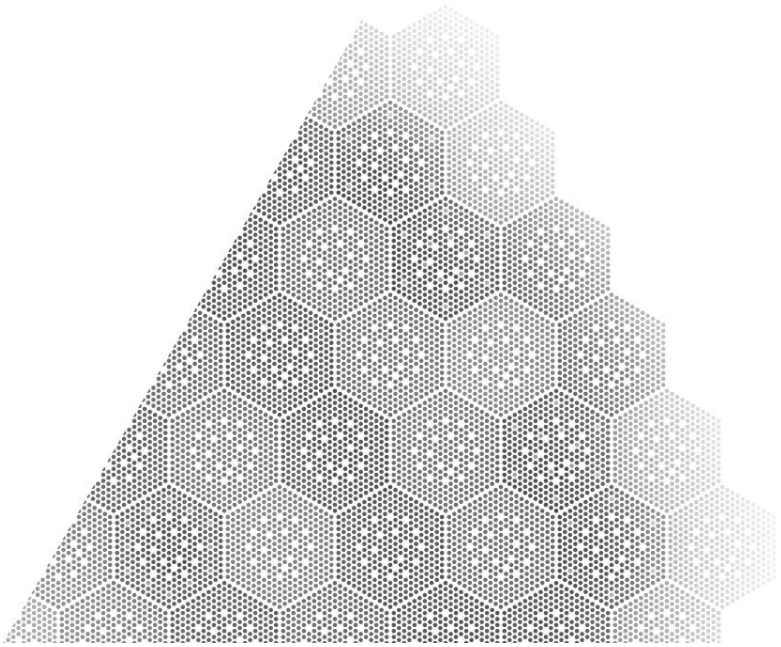

Figure 8. Transverse section (at z=6.23 cm from the core bottom) of the by pin defined fission neutron source distribution, averaged by the 8-th (stationary) company period, for 60° rotation symmetry sector.

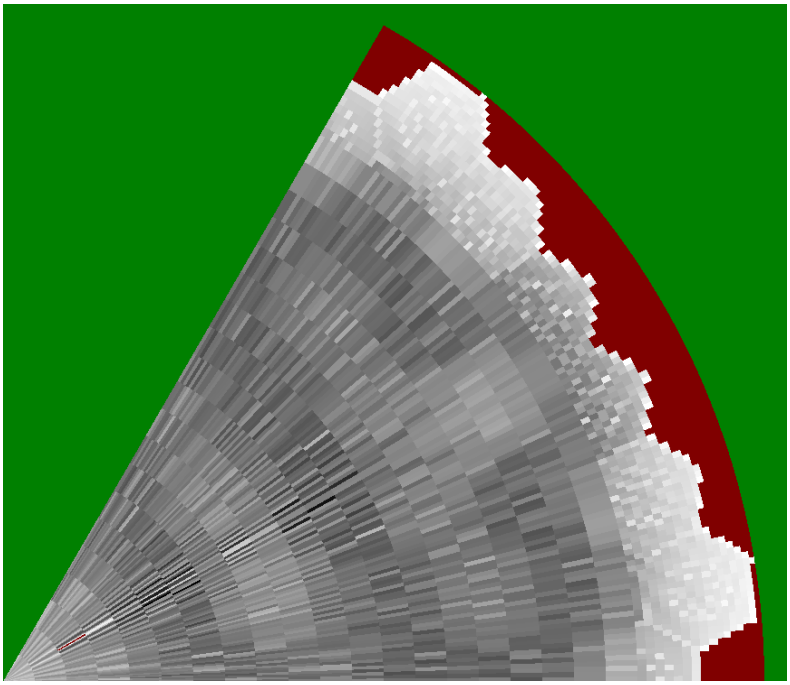

Figure 9. Transverse section (at z=6.23 cm from the core bottom) of the by pin defined fission neutron source distribution for the 8-th (stationary) company, converted on the mesh by ConSource code with conservation of the local neutron yield.

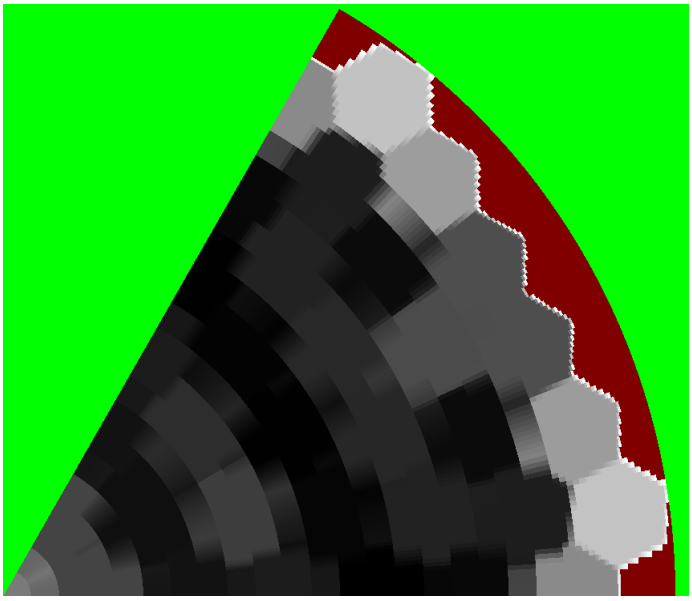

Figure 10. Transverse section (at z=6.23 cm from the core bottom) of the by assembly given fission neutron source distribution for the 8-th (stationary) company, converted on the spatial mesh by ConSource code with conservation of the local neutron yield.

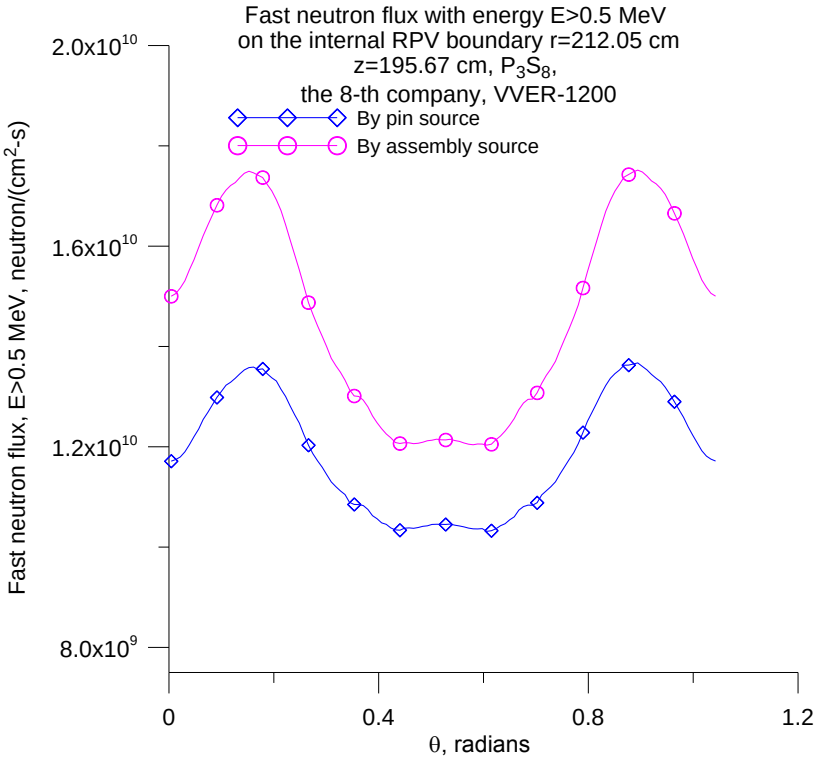

Figure 11. The ϑ variable distribution of the fast neutron flux with $E > 0.5\,\text{MeV}$ on the internal boundary of RPV $r = 212.05$ cm and z=195.67 cm (106.57 cm from the core bottom) for the 8-th company for by pin/by assembly defined source approximation used. The source is normalized to 2.761×10^{20} neutrons in the core. No surveillance specimen assemblies were accounted.

3.2. Computational Results

Numerical experiment has shown that the VF method provides acceptable approximation of the problem geometry. Coupled with the AWDD scheme it ensures sufficiently fast convergence in mesh refinement of calculated fast and thermal neutron fluxes, DPA and energy deposition profiles even in the vicinity of strong heterogeneities (baffle, surveillance specimen assemblies, channels for thermal neutrons ionization chambers, etc.). In radiation shielding calculations, where thick homogeneous regions are typically available, for well defined spatial mesh the number of cells with additional mixtures, generated by the VF method, is relatively small (about 5-8% for the problems solved) in comparison with the full core calculations, where above 50% of cells may contain additional mixtures and superconvergence effect, generated by the local balance conservation, ensured by the VF method use, takes place [5, 6]. But some improvement in the flux accuracy calculation, especially in strong heterogeneity regions, takes place in radiation shielding calculations also.

In Figs. 12 and 13 we present 2D r,ϑ geometry results of calculation of theta distributions of the fast neutron flux with E>0.1 MeV in the baffle region and in the vicinity of inner surface of RPV for z=201.7 cm transverse section of VVER-1200 geometry, received on 120 and 240 intervals spatial mesh in theta variable per 60° rotation symmetry sector (results for the first half of the sector are only depicted) with the use of the VF method and by a standard approach, where no additional mixtures are introduced and the local mass balance is not supported. From Figs. 12 and 13 it is possible to conclude that the VF method typically ensures some improvement in accuracy in comparison with the ordinary approach, where the local mass balance is not supported.

3D VVER-1200 radiation shield calculations provide required neutron and gamma-ray fluxes, fast neutron flux fluence, DPA and energy deposition profiles. As an example, in Figs. 14 and 15 results of 3D r,ϑ,z geometry P_3S_8 calculation of axial distribution of the fast neutron flux with $E > 0.5\,\text{MeV}$ and the velocity of DPA generation in the vicinity of internal surface of cladding ($r = 211.6$ cm), RPV ($r = 212.5\,\text{cm}$), internal boundary of the first ($r = 208.0$), the second and the third ($r = 208.25$) floor surveillance specimens for $\vartheta = 8.25°$ are depicted. From these results it is possible to conclude that there is some advance in fast neutrons fluence and DPA for the specimen internal surface iron regarding to the RPV internal surface one (1.49 and 1.61, respectively, for the first floor assembly specimens).

In Fig. 16 the results of the 3D calculation of the theta angle distribution of the thermal neutron flux with E<0.41399 eV in the vicinity of ionization chamber channels, located in the dry shield beyond the RPV, are depicted.

The code execution times required to perform 3D calculation for the 60° rotation symmetry sector of VVER-1200 for spatial r,ϑ,z mesh 218×120×175 = 4 578 000 cells, P_3S_8 approximation with inner iterations point-wise scalar flux convergence 10^{-3}, up-scattering iterations point-wise convergence 5×10^{-3} for serial version of KATRIN code for by assembly and by pin defined sources are 3 days 7 hours and 3 days 13.4 hours, respectively, for Intel Core 2 Duo E6600 PC supplied by 8Gb RAM and RAID 0 array with two HD.

The use of a preliminary variant (with no parallelization in the polar angle) of a parallel version of KATRIN code, based on 2D KBA algorithm and OpenMP interface, for 54×30 spatial decomposition in r,ϑ plane gives about 40% decrease in these times for two-core E6600 PC and about 4.3 times decrease for quad-core Intel Core i7-920 PC.

3.3. Fine Group Calculation Results

Results of calculations essentially depend on the accuracy of cross-section library used. The VVER-1200 baffle geometry was changed in comparison with the VVER-1000 one, and the VVER-1200 downcomer is 4.9 cm thicker than the VVER-1000 one. There are also other changes in the radiation shielding geometry. So, the accuracy of the problem dependent BGL1000 [14] cross-section library (with 47 neutron and 20 photon groups), generated from VITAMIN-B6 fine group library (with 199 neutron and 42 photon groups) by collapsing with VVER-1000 spectra, to be applied to the VVER-1200 radiation shielding calculations, may give rise some error. To estimate the quality of the BGL1000 cross-section library in performing VVER-1200 radiation shielding calculations, the fine group calculations of the problem with the use of the ABBN-93[15] (with 299 neutron and 15 photon groups) and CONSYST code [17] to prepare mixtures, and the new ENDF-B-VII and RUSFOND [16] based VITAMIN-B6 like libraries (with 199 neutron and 42 photon groups) by the synthesis method were performed. Some results of this investigation are presented.

In Figs. 17 and 18 results of calculation of the theta distribution of the fast neutron flux with $E > 0.5\,\text{MeV}$ in the vicinity of the internal $r = 212.05$ cm and external $r = 232.25$ cm boundaries of RPV, respectively, and z=195.67 cm (106.57 cm from the core bottom) for the 1-st company in dependence of cross-section library used are depicted. In these calculations the source was normalized to 2.6×10^{20} neutrons in the core and a preliminary geometry model with no surveillance specimen assemblies was used. In Table I the differences (in %) in the maximum of calculated by the synthesis method fine group theta distributions of the fast neutron flux with $E > 0.5$ MeV, DPA and thermal neutron flux with E<0.41399 eV in comparison with BGL1000 ones, are given. From Figs. 17 and 18, and Table I we can conclude that the use of the BGL1000 library essentially underestimate the fast neutron flux with $E > 0.5\,\text{MeV}$ and DPA on the external boundary of RPV in comparison with ENDF-B-VII and RUSFOND based VITAMIN-B6 like libraries. Some underestimation of the thermal neutron flux with E<0.41399 eV in the vicinity of VVER-1200 ionization chamber channels also takes place.

The use of the same geometry/source input by MCU [9] and KATRIN codes gives an opportunity to perform both Monte-Carlo and S_N transport calculations with the use of the same geometry/source model of the problem solved (see Fig. 19). This also simplifies implementation of the CADIS methodology [11] for using the 3D S_N adjoint fluxes for automatic variance reduction of Monte-Carlo calculations. The CADIS approach simplifies receiving of the high accuracy radiation shielding results, which can be applied for additional validation of multigroup cross-section libraries, used in S_N radiation shielding calculations.

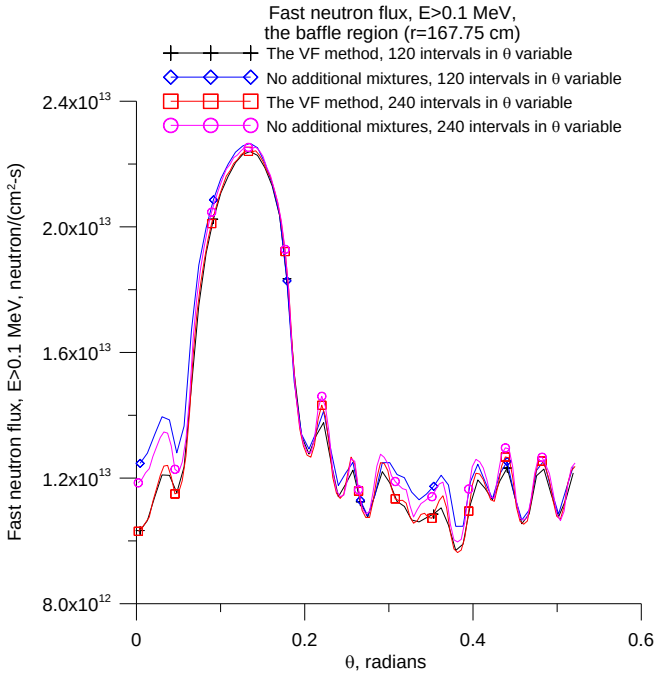

Figure 12. 2D r,ϑ geometry calculation of the theta dependence of neutron flux with E>0.1 MeV at $r=167.75$ cm (the baffle region) for z=201.7 cm transverse section of VVER-1200 geometry by the VF method and by the standard approach (no additional mixtures are used).

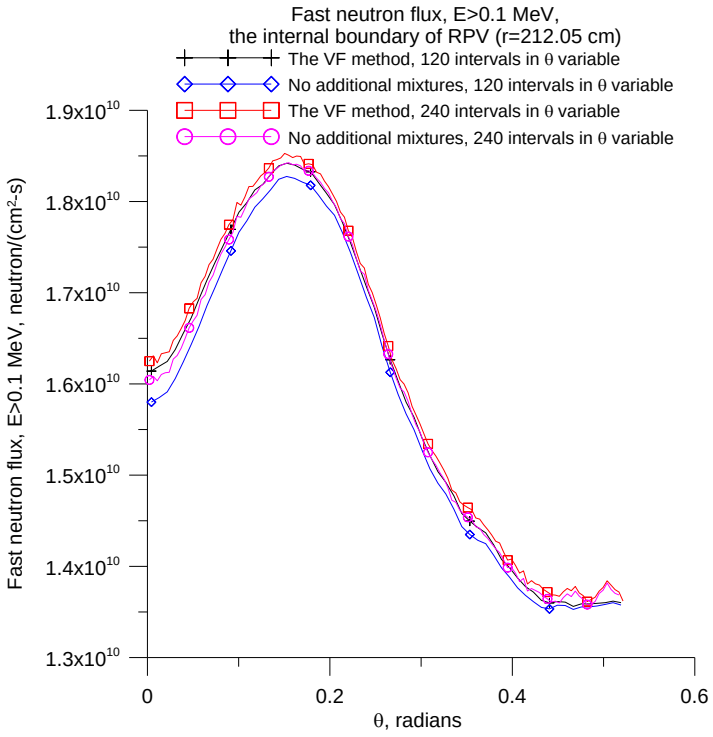

Figure 13. 2D r,ϑ geometry calculation of the theta dependence of neutron flux with E>0.1 MeV at $r=212.05$ cm (the internal boundary of RPV) for z=201.7 cm transverse section of VVER-1200 by the VF method and by the standard approach (no additional mixtures are used).

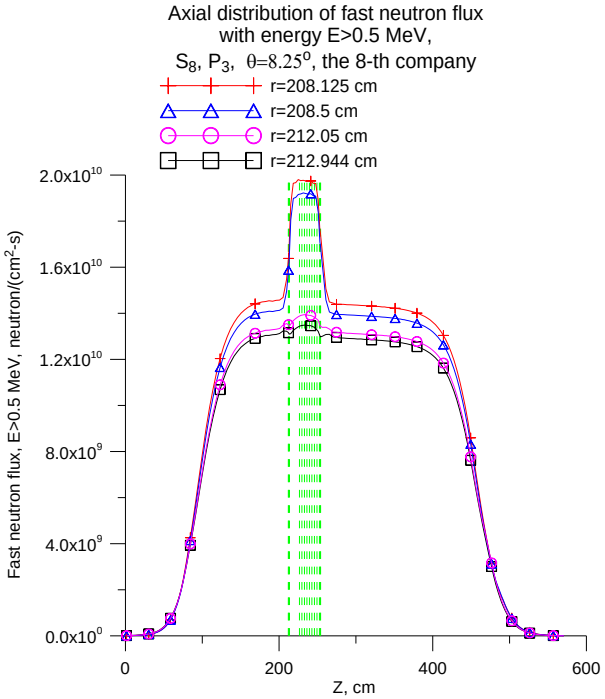

Figure 14. Axial distribution of the fast neutron flux with $E > 0.5\,\text{MeV}$ in the vicinity of the surveillance specimen assembly and the internal radius of the VVER-1200 RPV for $\vartheta = 8.25°$. The source is normalized to 2.55×10^{20} neutrons in the core.

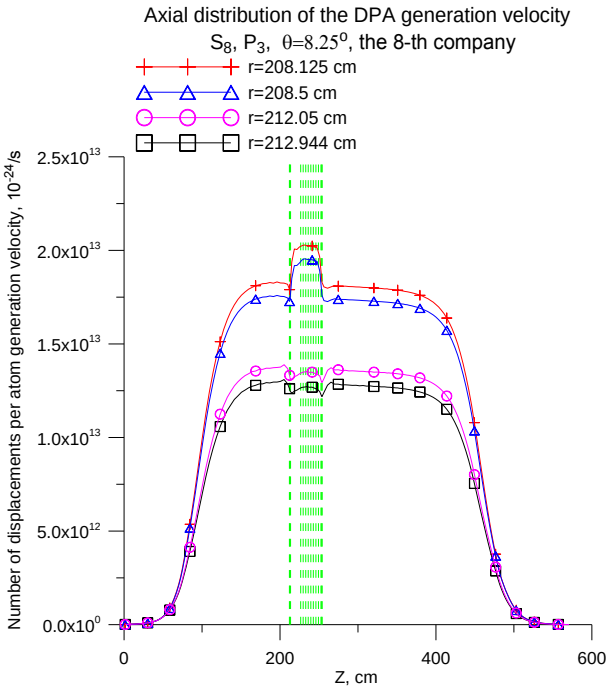

Figure 15. Axial distribution of the velocity of DPA generation in the vicinity of the surveillance specimen assembly and the internal radius of the VVER-1200 RPV for $\vartheta = 8.25°$. The source is normalized to 2.55×10^{20} neutrons in the core.

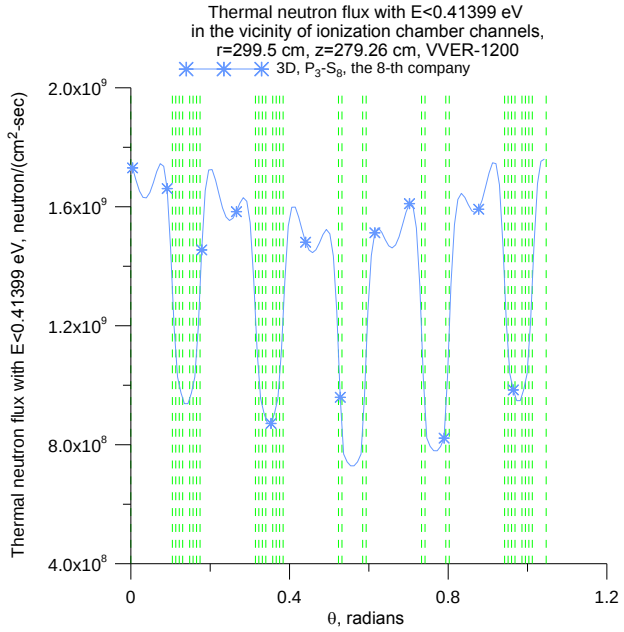

Figure 16. Results of the 3D P_3S_8 calculation of the ϑ variable distribution of the thermal neutron flux with E<0.41399 eV in the vicinity of VVER-1200 ionization chamber channels. The source is normalized to 2.55×10^{20} neutrons in the core.

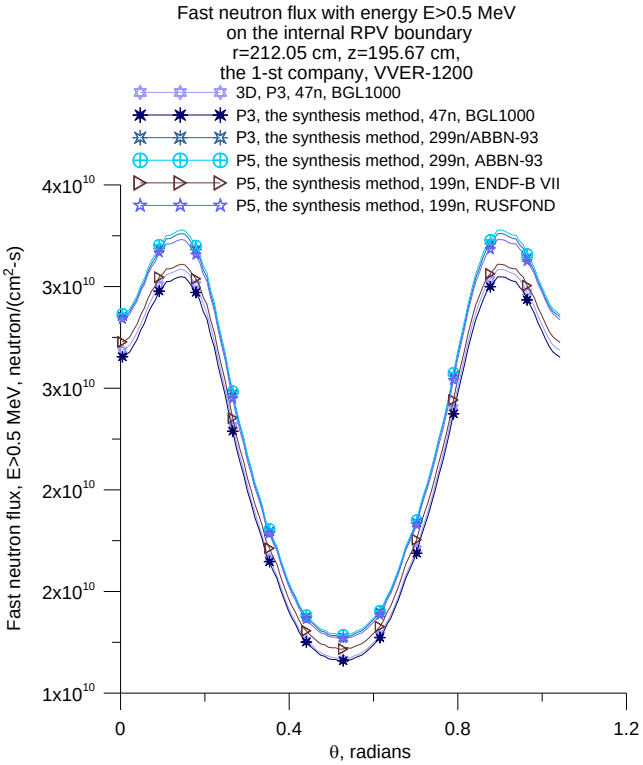

Figure 17. The theta distribution of the fast neutron flux with $E > 0.5$ MeV on the RPV internal boundary $r = 212.05$ cm and z=195.67 cm (106.57 cm from the core bottom) for the 1-st company in dependence of cross-section library used. No surveillance specimen units were used.

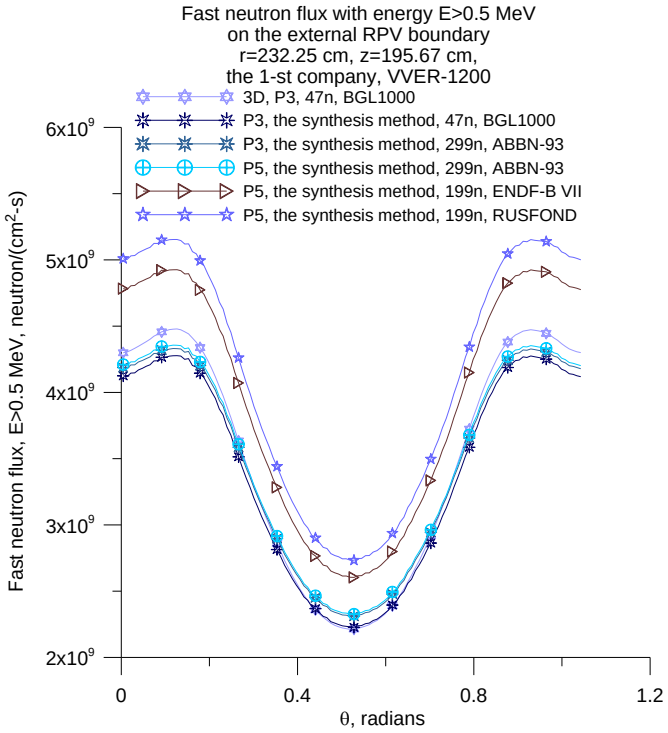

Figure 18. The theta distribution of the fast neutron flux with $E > 0.5$ MeV on the external boundary of RPV $r = 232.25$ cm and z=195.67 cm (106.57 cm from the core bottom) for the 1-st company in dependence of cross-section library used. No surveillance specimen units were used.

Table I. Differences in the maximum of calculated by the synthesis method the fine group theta distributions of the fast neutron flux with $E > 0.5$ MeV, DPA and thermal neutron flux with E<0.41399 eV in comparison with BGL1000 ones, %.

Fine group cross-section library	CONSYST/ ABBN-93 $299n+15\gamma$	TRANSX/ ENDF-B VII $199n+42\gamma$	TRANSX/ RUSFOND $199n+42\gamma$
Internal boundary of RPV, r =212.05 cm			
Fast neutron flux, $E > 0.5$ MeV, %	7.5	2.6	6.25
DPA, %	9.6	1.7	4.8
External boundary of RPV, r =232.25 cm			
Fast neutron flux, $E > 0.5$ MeV, %	1.8	15.9	20.6
DPA, %	3.0	9.6	13.2
The centre of ionization chamber channel, r =299.5 cm, $\vartheta = 8°$			
Thermal neutron flux, $E < 0.41399$ eV, %	7.0	20.0	26.0

4. CONCLUSIONS

We have found that Monte-Carlo code based tracing algorithm can be efficiently applied for converting combinatorial presentation of the problem geometry and source to a bit-mapped one with local conservation both the mass of original materials (within the framework of the VF

method) and the source yield for every spatial cell of the mesh. The received geometry and source approximations, being applied for radiation shielding calculations, improve accuracy of calculated flux distributions in comparison with an ordinary approach, where local mass balance is not supported. It is also important that implementation of the VF method requires only minor changes in S_N transport codes, working with regular orthogonal meshes. To ensure required accuracy of the VVER-1200 radiation shielding calculations the new problem dependent cross-section library should be developed. It seems also that the available BGL440 and BGL1000 problem dependent cross-section libraries [14] should be updated with the use of the last versions of evaluated nuclear data libraries. Developed geometry and source converters, coupled with geometry visualization tools (MCU Viewer and Maplook script), parallel version of KATRIN code and KATRIF postprocessor [10], make high-accuracy 3D S_N VVER radiation calculations less time consuming for multicore PC/servers, reserving the approximate synthesis method for fine group calculations.

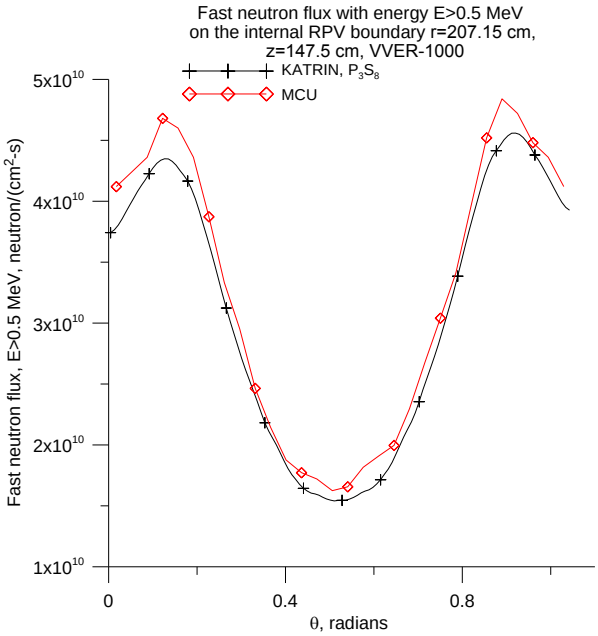

Figure 19. Results of calculation of the theta distribution of the fast neutron flux with $E > 0.5$ MeV on the internal boundary of VVER-1000 RPV, Balakovo 3 Unit, the 5-th company.

REFERENCES

1. T. A. Wareing, J. M. McGhee, D. A. Barnett and G. A. Failla, "ATTILA Calculations for the 3-D C5G7 Benchmark Extension," *Proc. of International Conference on Mathematics and Computation, Supercomputing, Reactor Physics and Nuclear and Biological Applications*, Avignon, France, Sept. 12-15, 2005, on CD-ROM.
2. J. A. Dahl and R. E. Alcouffe, "PARTISN Results for the C5G7 MOX Benchmark Problems," TANS, **89**, 274 (2003).
3. J. A. Dahl, "3-D Extension C5G7 MOX Benchmark Results Using PARTISN," *Proc. of International Conference on Mathematics and Computation, Supercomputing, Reactor*

Physics and Nuclear and Biological Applications, Avignon, France, Sept. 12-15, 2005, on CD-ROM.
4. P. Humbert, "Results for the C5G7 3-D Extension Benchmark Using the Discrete Ordinates Code PANDA," ibid.
5. M. I. Gurevich, D. S. Oleynik, A. A. Russkov and A. M. Voloschenko, "About the Use of the Monte-Carlo Code Based Tracing Algorithm and the Volume Fraction Method for S_N Full Core Calculations," *Proc. of International Conference Advances in Nuclear Analysis and Simulation – PHYSOR 2006*, Vancouver, Canada, September 10-14, Paper D062, pp. 1-10, 2006, on CD-ROM.
6. A. M. Voloshchenko, A. A. Russkov, M. I. Gurevich, D. S. Oleynik, "About the Use of Approximations, which Ensure Mass Balance Conservation by Spatial Meshes, in S_N Full Core Calculations," *Atomic Energy*, **104**, No. 5, 264-269, 2008.
7. R. Orsi, "A General Method of Conserving Mass in Complex Geometry Simulations on Mesh Grids and Its Implementation in BOT3P5.0," *Nucl. Sci. Eng.*, **154**, 247–259 (2006).
8. R. Orsi, "BOT3P Version 5.1: A Pre/Post-Processor System for Transport Analysis," *ENEA report FIS-P9H6-014*, Italy, 2006.
9. L. P. Abagian, A. E. Glushkov, E. A. Gomin, S. S. Gorodkov, M. I. Gurevich, M. A. Kalugin, L. V. Mayorov, S. V. Marin, D. S. Olejnik, D. A. Shkarovsky, M. S. Yudkevich, "MCU-REA/2 with Data Bank DLC/MCUDAT-2.2," Editors: E. A. Gomin, L.V. Maiorov. *Report of RRC Kurchatov Institute* No. 36/17-2006, Moscow (2006).
10. "The CNCSN: One, Two- and Three-Dimensional Coupled Neutral and Charged Particle Discrete Ordinates Code Package," *RSICC code package CCC-726*, 2008 (the abstract is online: http://rsicc.ornl.gov/codes/ccc/ccc7/ccc-726.html, http://www.nea.fr/abs/html/ccc-0726.html).
11. J. C. Wagner, A. Haghighat, "Automated Variance Reduction of Monte Carlo Shielding Calculations using the Discrete Ordinates Adjoint Function", *Nucl. Sci. Eng.*, **128**, pp. 186-208 (1998).
12. A. M. Voloschenko, "Consistent P_1 Synthetic Acceleration Scheme for Transport Equation in 3D Geometries," *Proc. of International Conference on Mathematics and Computation, Supercomputing, Reactor Physics and Nuclear and Biological Applications*, Avignon, France, September 12-15, Paper 070, pp. 1-37, 2005, on CD-ROM.
13. A. M. Voloshchenko, "KP_1 Acceleration Scheme for Inner Iterations Consistent with the Weighted Diamond Differencing Scheme for the Transport Equation in Three-Dimensional Geometry," *Comp. Math. & Math. Phys.*, **49**, No. 2, pp. 334–362 (2009).
14. J. Bucholz, S. Antonov, S. Belousov, "BGL440 and BGL1000 Broad Group Neutron/Photon Cross Section Libraries Derived from ENDF/B-VI Nuclear Data", *IAEA*, INDC(BUL)-15, April 1996.
15. G. N. Manturov, M. N. Nikolaev and A. M. Tsiboulia, "ABBN-93 Group Data Library, Part1: Nuclear Data for the Calculations of Neutron and Photon Radiation Fields," Vienna, *IAEA*, INDC(CCP)-409, 1997.
16. S. V. Zabrodskaya, A. V. Ignatyk, V. N. Koshcheev et al. "RUSFOND - Russian National Library of Evaluated Neutron Data," *Vopr. At. Nauki Tekh. Ser. Yadern. Const.*, No. 1&2 (2007).
17. G. N. Manturov, M. N. Nikolaev and A. M. Tsiboulia, "CONSYST Code for Constants Preparation. Description of Appliance," *Preprint IPPE-2828, Institute of Physics and Power Engineering* (2000) (in Russian).